Optical Metrology for Testing an All-Composite 2-Meter Diameter Mirror

Brian Catanzaro[a*], James A. Thomas[b], Don Small[b], Roger Johnston[b], Dan Barber[b], Steven Connell[c], Shaun Whitmore[c], and Eri Cohen[d]

[a]CFE Services, 5147 Pacifica Dr, San Diego, CA 92109
[b] Light Works Optics, Inc., 2691 Richter Ave., Suite 105, Irvine CA 92606
[c]Composite Optics Incorporated, 9617 Distribution Ave, San Diego, CA 92121
[d] Jet Propulsion Laboratory, California Institute of Technology,
4800 Oak Grove Drive, Pasadena CA 91109

ABSTRACT

The Herschel Space Observatory (formerly known as FIRST) consists of a 3.5 m space telescope designed for use in the long IR and sub-millimeter wavebands. To demonstrate the viability of a carbon fiber composite telescope for this application, Composite Optics Incorporated (COI) manufactured a fast (F/1), large (2 m), lightweight (10.1 kg/m^2) demonstration mirror. A key challenge in demonstrating the performance of this novel mirror was to characterize the surface accuracy at cryogenic (70 K) temperatures. A wide variety of optical metrology techniques were investigated and a brief survey of empirical test results and limitations of the various techniques will be presented in this paper. Two complementary infrared (IR) techniques operating at a wavelength of 10.6 microns were chosen for further development: (1) IR Twyman-Green Phase Shifting Interferometry (IR PSI) and (2) IR Shack-Hartmann (IR SH) Wavefront Sensing. Innovative design modifications made to an existing IR PSI to achieve high-resolution, scannable, infrared measurements of the composite mirror are described. The modified interferometer was capable of measuring surface gradients larger than 350 microradians. The design and results of measurements made with a custom-built IR SH Wavefront Sensor operating at 10.6 microns are also presented. A compact experimental setup permitting simultaneous operation of both the IR PSI and IR SH tools is shown. The advantages and the limitations of the two key IR metrology tools are discussed.

Keywords: IR Metrology, Phase Shifting Interferometry, Shack-Hartmann Sensor, Carbon Fiber Composite, Space Telescope, Curvature Sensor, Foucault Test, KRS-5

1. INTRODUCTION

The Herschel Space Observatory (formerly known as FIRST), is a European Space Agency (ESA) cornerstone mission, that will be used for photometry, imaging and spectroscopy in the 80 to 670 μm range (see Figure 1). The key science goals that this observatory will achieve concern how galaxies formed in the early universe, and how stars form, and have been forming, throughout the history of the universe. NASA, through the Jet Propulsion Laboratory (JPL), has contributed to the telescope and its design. This paper will discuss the work done by JPL, Composite Optics, Incorporated (COI), and Light Works Optics, Incorporated (LWO) to develop optical metrology instruments to characterize a large aperture (2 m) demonstration mirror at 70 K. Requirements traceable to the Herschel Space Observatory are wavefront error (6 μm RMS), mass (280 kg), primary mirror diameter (3.5 m), F-number (F/0.5), and the operational temperature (70 – 90 K).

* Correspondence: Email: bcatanza@alumni.caltech.edu; Telephone: 858 204 6299;

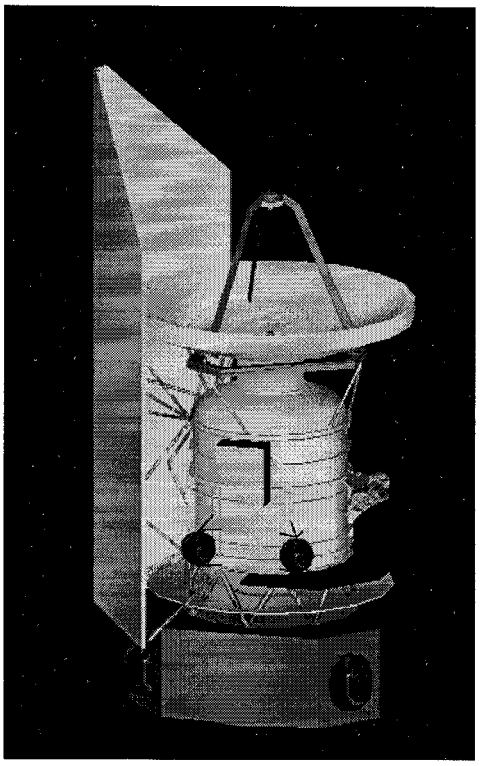

Figure 1: Herschel Space Observatory

In response to the telescope requirements a low mass, low coefficient of thermal expansion (CTE) telescope [1] has been designed using carbon fiber reinforced polymer (CFRP) and a 2 m diameter demonstration mirror was fabricated [2] for the purpose of cryogenic performance characterization. The 2 m diameter demonstration mirror is spherical in shape with a radius of curvature of 4.2 m. It is coated with a protected gold and has an areal density of 10.1 kg/m^2. The mirror is a unique, segmented facesheet. The core that supports the facesheet is contiguous, but the facesheet is separated into six (6) petals. A specific goal for the demonstration mirror was the optical characterization of surface errors at 70 K.

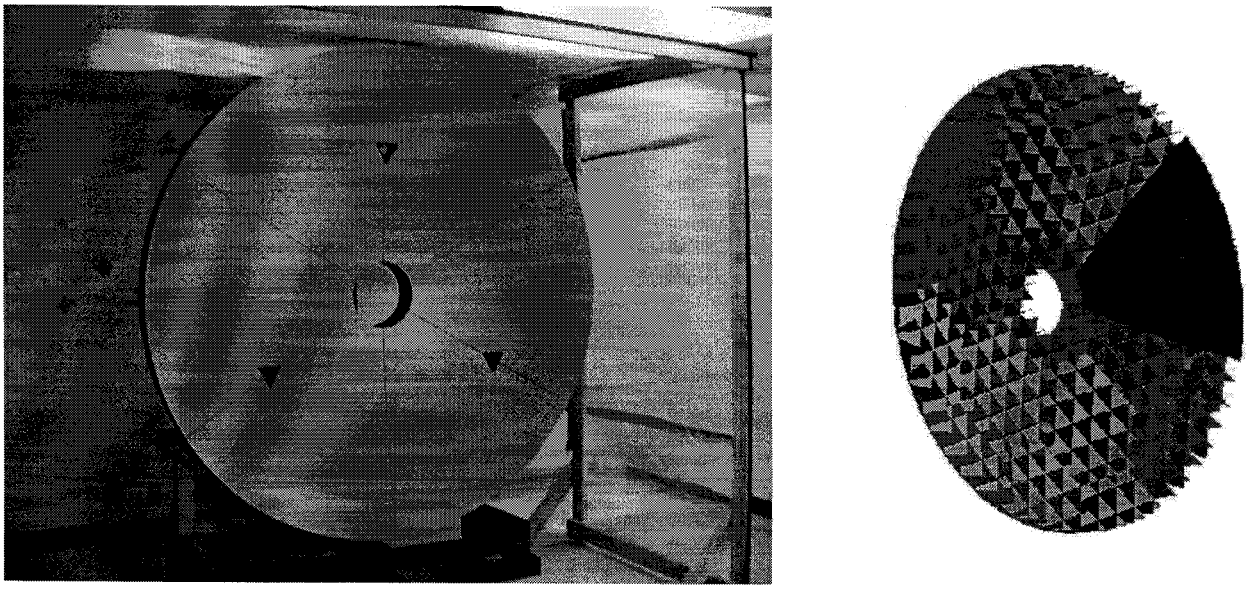

Figure 2: 2 m CRFP Lightweight Demonstration Mirror (10.1 kg/m^2)

Several features of the carbon fiber 2 m mirror differentiate it from traditional mirrors. [2] The material, CFRP, is an extremely low expansion material even at cryogenic temperatures. The manufacturing process involved curing the facesheets on a mold in order to generate a smooth near net shape surface and an assembly technique that created the final figure of the mirror. Although the manufacturing mold was polished, the mirror itself was never polished. The stiffness of the mirror met all of the launch requirements traceable to the Herschel Space Observatory. However, it was sufficiently lightweighted that gravity did affect the surface figure. Generally the surface figure was specular (surface roughness: < 0.6 μm RMS from profilometry data). Material uniformity was closely controlled and bond lines were minimized to ensure minimal quilting upon exposure to cryogenic temperatures. However, some quilting was anticipated.

The requirements for metrology of the surface were to support the Herschel Space Observatory flight telescope test requirements. These requirements are summarized as follows:

- Measure surface deformation as a function of cryogenic exposure (room temperature to 70 K),
- Report surface peak to valley (PV) and RMS,
- Sample the mirror surface sufficiently to generate Zernike coefficients 1 – 36,
- Sample the mirror surface sufficiently to characterize effects from quilting and the gaps between the petals.

The accuracy for these measurements was required to support the 6 μm RMS wavefront error (WFE) for the telescope as well as an encircled energy specification and a stray light specification. Given the WFE specification of 0.6 μm RMS, an allocation of 0.5 μm RMS was assigned to the metrology accuracy. Although the majority of the stray light specification was not related to interferometric surface error measurement, one specific portion of the specification was related to mid-spatial frequency errors. [3]

Work testing CFRP mirrors [4, 5, 6] indicated that an infrared interferometer was a useful tool for measurement. However, due to the temperatures involved (i.e. 70 K) and based on prior test results on this 2 m demonstration mirror [2], all relevant optical metrology methods were reviewed. Two techniques were selected in order to increase the likelihood of a successful measurement. In order to support these techniques, two existing instruments were redesigned and optimized for this test: an infrared interferometer (IR PSI) and an infrared Shack-Hartmann (IR SH) wavefront sensor. Modifications and upgrades to the optics, detection, and software were performed. A configuration that allowed both instruments to view the mirror during the test was designed. Data was collected and the limits of these instruments were explored.

2. REVIEW OF OPTICAL METROLOGY TECHNIQUES

The challenge of a unique lightweight mirror and the test environment inspired a survey of optical metrology techniques. The techniques considered were: Foucault testing [7], Curvature Sensing [8, 9], Wavefront Reconstruction [10, 11], Profilometry, Interferometry [7], and Shack-Hartmann Wavefront Sensing [12]. The basis for comparison was

- Support of PV/RMS WFE (6 μm RMS),
- Dynamic range sufficient to capture all surface errors relevant to the telescope requirements (<870 μrad – derived from telescope requirements)
- Compatibility with surface errors anticipated for the 2 m demonstration mirror
- Instrument development time
- Heritage for large, fast mirror measurement at cryogenic temperatures

Table 1 is a summary of the comparison.

Table 1: Comparison of Metrology Techniques for Cryogenic Measurement of a Large, Fast CFRP Mirror

Technique	Supports PV/RMS Req.	Dynamic Range for Quilting	Compatibility with Mirror Technology	Instrument Development Time	Heritage for Cryo Space Telescopes
Foucault (Knife Edge)	Basic Technique is Qualitative	Basic Technique is Qualitative	Best Done at 80 μm	Months for Numerical Instrument	Many Ground Telescopes
Curvature Sensing	Nominally Supports PV/RMS	Generally Sensitive to Quilting	Best Done at 80 μm	Months for this Mirror Technology	Some Ground Telescopes
Phase Retrieval	Nominally Supports PV/RMS	Generally Sensitive to Quilting	Best Done at 80 μm	Months for this Mirror Technology	Considered for NGST
Profilometry	Supports PV/RMS	Sufficient Dynamic Range	Yes	Existing Technology for Room Temp.	Not Compatible with Cryo
Interferometry	Supports PV/RMS	Generally Sensitive to Quilting	10.6 μm Instrument Needs Engineering	Weeks for this Mirror Technology	Cyro Test Heritage
Shack-Hartmann	Supports PV/RMS	Generally Sensitive to Quilting	0.6 μm Instrument Needs Re-Engineering	Weeks for this Mirror Technology	Some Ground Telescopes

1. Foucault Testing

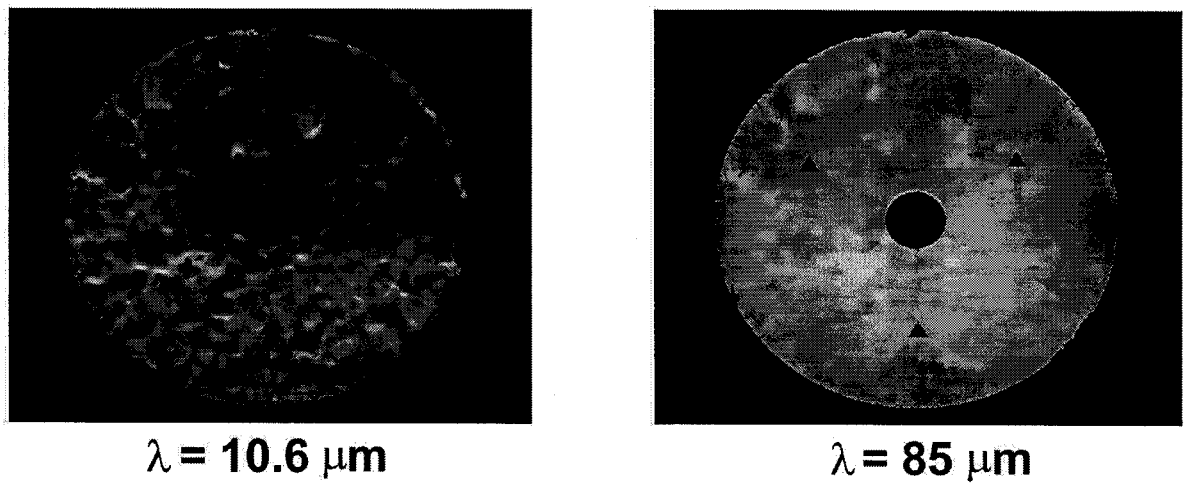

Figure 3: Simulated Foucault Test

Foucault (knife edge) testing is a well-known classic optical test. The test involves a knife edge placed at focus that obscures light rays that do not pass through the focus. This test works particularly well for diffraction limited optics illuminated at

their operating wavelength. By moving the knife edge above and below the focal point, the knife edge acts like a low-pass filter. Slopes higher than that of the cutoff frequency, determined by the location of the knife edge and the focal length of the mirror, are blocked. The following equation describes the cutoff frequency:

$$v_{cutoff} = \frac{x_{knife}}{\lambda \times f_{mirror}},$$

where v_{cutoff} is the maximum spatial frequency passing by the knife edge, x_{knife} is the distance between the optical axis and the knife edge, λ is the wavelength of illumination and f_{mirror} is the focal length of the mirror. Generally the method has been used qualitatively. With careful calibration, it has been used for quantitative evaluation. [7] However, this method has several drawbacks when applied to mirrors for the Herschel Space Telescope and specifically the 2 m demonstration mirror. First, the shortest wavelength that the telescope is specified for is 80 μm. The mirror was expected to be diffraction limited at this wavelength, but no practical source was available. Therefore the mirror would have to be tested at a wavelength much shorter than the diffraction limit. Figure 3 is an image of a Foucault test performed on the 2 m demonstration mirror using visible light and a simulated Foucault image using the operating wavelength. This method had insufficient heritage for cryogenic flight telescopes and lacked a mature methodology for quantitative measurement.

2. Curvature Sensor

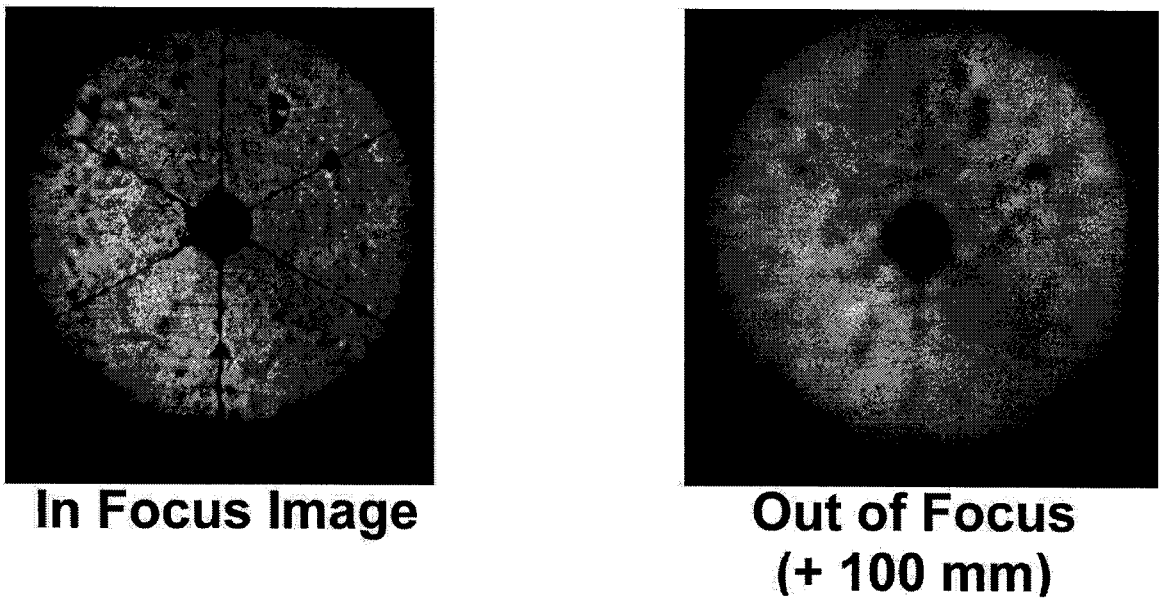

Figure 4: Pupil Using Visible Light (λ = 0.6 μm)

The Curvature Sensing method uses in and out of focus pupil image patterns to reconstruct the phase of the mirror. Recently, this technique has been used on ground observatories to measure wavefronts for an adaptive optics system. [9] The technique is capable of analyzing highly aberrated wavefronts (10's to 100's λ) and does not require reference optics (i.e. flats, test spheres) or a coherent light source. The technique relies on changes in intensity as a function of distance from the mirror; increasing intensity in a portion of the image indicates a locally converging wavefront, decreasing intensity indicates a locally diverging wavefront. Figure 4 shows an image of the focal spot of the mirror at and through focus. A relatively small blur circle must be formed and imaged onto a sensor. Scattering from the surface roughness and lack of pupil definition caused these images to be unprocessable. Infrared illumination would have reduced scattering, but test was not tried. With adjustments to the optical system for recording the pupil images, this method may have resulted in satisfactory performance. Although there is hope that this technique will become more widely used, the following additional concerns should be mentioned. The instrumentation for this technique though simple, is new. Sources of error are not well understood, there is

insufficient heritage to support cryogenic flight telescopes and the technique lacks a mature methodology for quantitative measurement.

3. Phase Retrieval

Phase Retrieval also uses in and out of focus intensity patterns to reconstruct the phase of the mirror. Wavefront sensing is performed using focus-diverse, iterative transform phase retrieval. This starts by taking two or more images, defocussed enough to spread the light over a large number of pixels (20-200, depending on required sensitivity and desired spatial frequency resolution). Typically 3 images, one in focus and 2 taken on opposite sides of focus, are used. These images are processed using a modified Gerchberg-Saxton (G-S) algorithm. [10] The G-S iteration starts with a random guess at the phase of the pupil used to form the image. This is combined with the square-root of the amplitude of the image data to create an estimate of the image. This is inverse Fourier transformed back to pupil space, and then the phase due to the diversity factor (the defocus) is removed, and the aperture mask is applied. The result is an estimate of the in-focus pupil. Then the diversity factor is put back in and the result is Fourier transformed back to the image plane. The phase from this estimated image-plane field is combined with the square root of the data to start the next iteration. The instrumentation has similar advantages and limitations as the Curvature Sensor. This technique achieves better convergence for small aberrations ($<<1$ wave), which is expected at $\lambda = 80$ μm. Unfortunately, sources and sensors for this type of measurement are not practical at $\lambda = 80$ μm.

4. Profilometry

There are several profilometry (CMM) facilities capable of measuring the surface of this optic accurately. The stiffness of the substrate requires distributed support (e.g air bag, whiffle tree, actuators) to measure in simulated 0-g or it requires several orientations, some incompatible with CMM configurations. Measurements were conducted at room temperature. Unfortunately, a non-idealized mount of the mirror caused errors in the measurement. Once these systematic errors were removed, there was correlation between room temperature interferometric measurements and the CMM measurement. However, none of the existing instrumentation is compatible with the 70 K test temperature requirement.

5. Interferometry

Interferometry is a well-recognized method of optical measurement. In particular, Fizeau and Twyman-Green phase shifting interferometers have been integrated into several commercial products (e.g. Zygo, Wyko, Phase Shift, et. al.). Given the surface deformations anticipated at cryogenic temperatures, wavelengths closer to the operating wavelength were preferred. Unfortunately, the wavelength closest to the operating wavelength in a commercial instrument was 10.6 μm; 8X shorter than the 80 μm operating wavelength. Infrared interferometers have been used to characterize several CFRP reflectors; [4, 5, 6] some of these reflectors have even been measured at extremely cold temperatures. A drawback of this technique is its sensitivity to vibration and limited measurement range. Interferometers are limited by the maximum fringe spacing that can be recorded by the sensor. This places a limit on the maximum recordable slope error. A commercial instrument manufactured by Breault Research Organization, Inc. (BRO) in the late 1980's was identified as a candidate metrology instrument. However, there were several deficiencies in the instrument: poor lateral resolution, notable astigmatism in images of fringes, and an outdated software and control hardware (computer) platform.

6. Shack-Hartmann Wavefront Sensing

The Shack-Hartmann Wavefront Sensor has recently gained acceptance as a method of optical metrology. This technique is a variation of the Hartmann screen test, using lens arrays instead of a mask with an aperture array. Beams created by the lens array essentially ray-trace the optical test configuration and slope errors in the test wavefront cause the focal spots to deviate from their ideal locations. These deviations are converted from slopes into a surface map. It has been compared to interferometry in terms of accuracy and has a larger dynamic range. It has recently been used for cryogenic mirror testing by NASA for the NGST program. [13, 14] Several sensors are commercially available (AOA Incorporated, Wavefront Sciences, et. al.) which include both hardware for capturing data and software for data analysis. Due to the centroiding nature of calculating the ray intercepts with the image sensor, the technique is relatively insensitive to vibration. However, the technique has a much lower lateral resolution than interferometry. It also requires that the wavefront be isoplanatic over the sampling area of a single lens in the array.

Due to the cost and resources involved in the test, a single cryogenic test was desired. The performance of the 2 m demonstration mirror at 70 K was unknown at the time of selection of the instruments. To ensure adequate data was

collected, two instruments were selected: the IS PSI and the IS SH sensor. These two instruments had the most heritage and had multiple options for commercial supply. With modification it was anticipated that at least one, if not both, would meet the requirements for measurement dynamic range and accuracy.

3. INFRARED PHASE SHIFTING TWYMAN-GREEN INTERFEROMETER

As mentioned previously, an infrared phase shifting interferometer (IR PSI) manufactured by BRO was available equipment for this test. However, the equipment had not been updated since the late 1980's and the resolution was clearly inadequate. [2] Several modifications were made the to IR PSI in order to create an instrument capable of fulfilling the requirements.

The instrument uses a line narrowed CO_2 source with a coherence length in excess of 10 m. The interferometer was configured as an unequal path system with a piezo driving the phase shifting reference mirror. The pupil was imaged to a pyroelectric vidicon (PEV) using a telescope with multiple magnifications (1X, 2X, 4X). The software, ISYS, was capable of data collection, surface map generation, and Zernike decomposition.

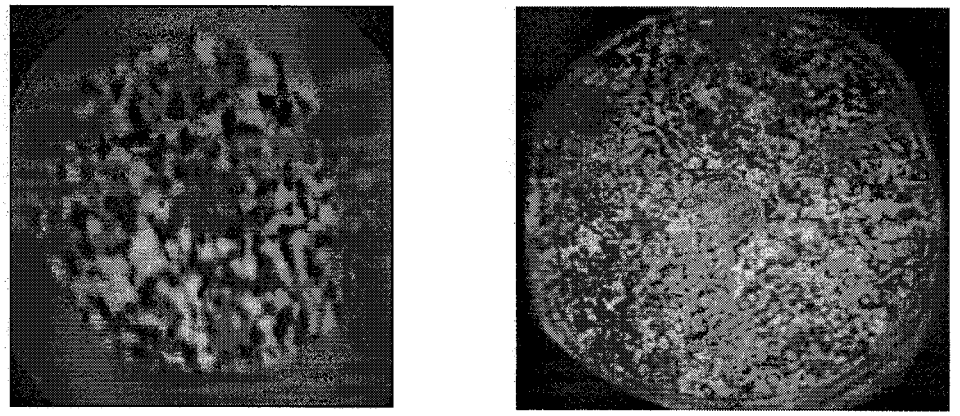

Figure 5: Interferograms of the 2 m Demonstration Mirror Before (Left) and After (Right) Modifications to the IR PSI

The modifications to the IR PSI were to the software, objective lens, sensor, and optics train. Figure 5 shows interferograms of the 2 m demonstration mirror before and after the modifications.

1. Software

The ISYS software was replaced by Intelliwave™ from Engineering Synthesis Design. Intelliwave has several features invaluable to this test. It has the capability to generate the first 36 Zernike coefficients and subtract any combination of these from the surface map. This allowed for specific analysis of spherical, astigmatic, and coma terms as well as rapid assessment of higher order (quilting) aberrations. Five (5) choices of phase shifting algorithms were available. In addition, phase angles and modulation could be represented graphically for each surface. This aided in calibrating the piezo stepping and overall stability of the test environment. Several phase unwrapping algorithms were implemented, including a very robust minimum gradient descent algorithm capable of unwrapping the phase on very dense fringes. The software also featured a quality control option that would screen test data and automatically reject data deemed unacceptable. All of these features were integrated into a programming language capable of automating the data collection. This enabled averaging of large sets (30) of surfaces, significantly reducing random noise errors in the surfaces.

2. Objective Lens

A custom objective lens was designed for use with the 2 m demonstration mirror (see Figure 6). The primary purpose of the custom objective is to allow full aperture interferometry and high resolution sub-aperture interferometry to be collected over the entire aperture without repositioning the interferometer. An additional benefit of the new design was an improvement in the lateral resolution. The improvements in the lateral resolution enabled higher fringe densities to be captured by the IR PSI. This was accomplished by designing a custom air-spaced doublet using spherical ZnSe lenses. One method of examining a high resolution portion of the wavefront of an optical system is to use a slow objective lens and translate/rotate the interferometer to point it to a different portion of the converging wavefront. The rotating window in the custom lens

objective enabled this capability without realigning the interferometer, resulting in a large timesaving in data collection. The scanning feature was implemented using a Germanium window positioned in a mount with two degrees of freedom: tilt and azimuthal rotation. As the window is rotated the collimated output of the interferometer is scanned over the clear aperture of the objective, resulting in a converging F/2 beam that can be steered to any position within the full F/1 cone supported by the objective's clear aperture.

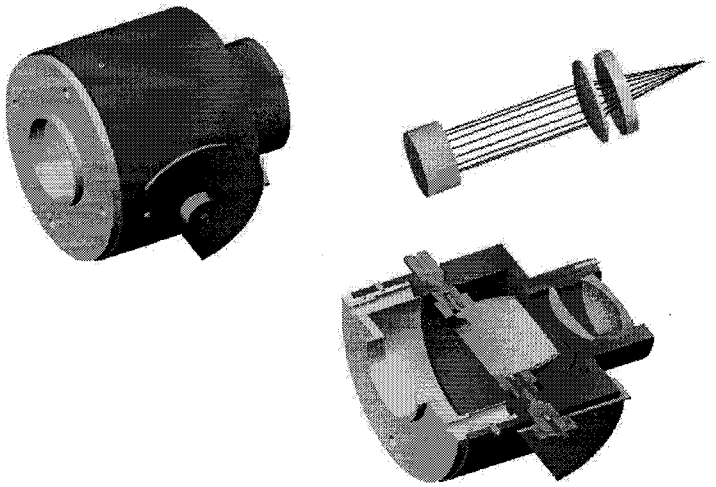

Figure 6: Custom Lens Objective

3. Sensor

The PEV was replaced by an Infrared Components Corporation (ICC) microbolometer array camera. This camera uses a new room temperature VO_2 resistive microbolometer technology. The resolution of the array is 320 x 240 and the output is 30 frames per second standard NTSC video. The sensor active area was close enough to the PEV that replacement was a simple mechanical modification. The microbolometer array had a much higher contrast and signal to noise ratio than the PEV. Another important factor was the real time imaging of the microbolometer array. The PEV operated on a time varying thermal signal. Therefore, in order to see an image of the interferogram, either the beam had to be chopped or the piezo-driven mirror had to be continuously sweeping.

4. Optics Train

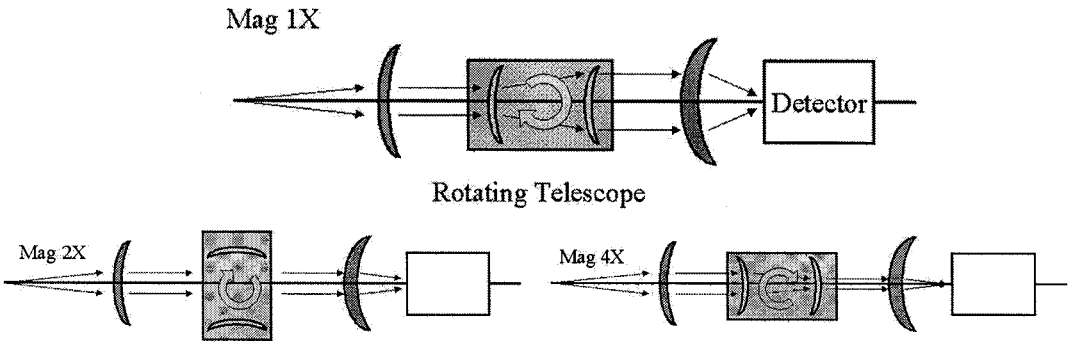

Figure 7: Relay Telescope Configurations

The interferometer optical system required minor modifications to improve the resolution. The telescope for relaying the fringe pattern to the sensor operated in three modes: pass through, forward, and reverse to provide 1X, 2X, and 4X magnification (see Figure 7). The lens positions were optimized to meet two goals: match the size of the active area on the sensor and provide the necessary magnification for low and high resolution interferometry. The original design of the IR PSI incorporated a static position for the sensor. This resulted in reducing the resolution of the magnified images of the fringe patterns. Instead, two jigs were designed to allow the sensor to be repeatably repositioned for each magnification. This resulted in significant improvements to the system. An additional modification was the insertion of a wedge to remove astigmatism in the original design. A photograph of the modifications is shown in Figure 8.

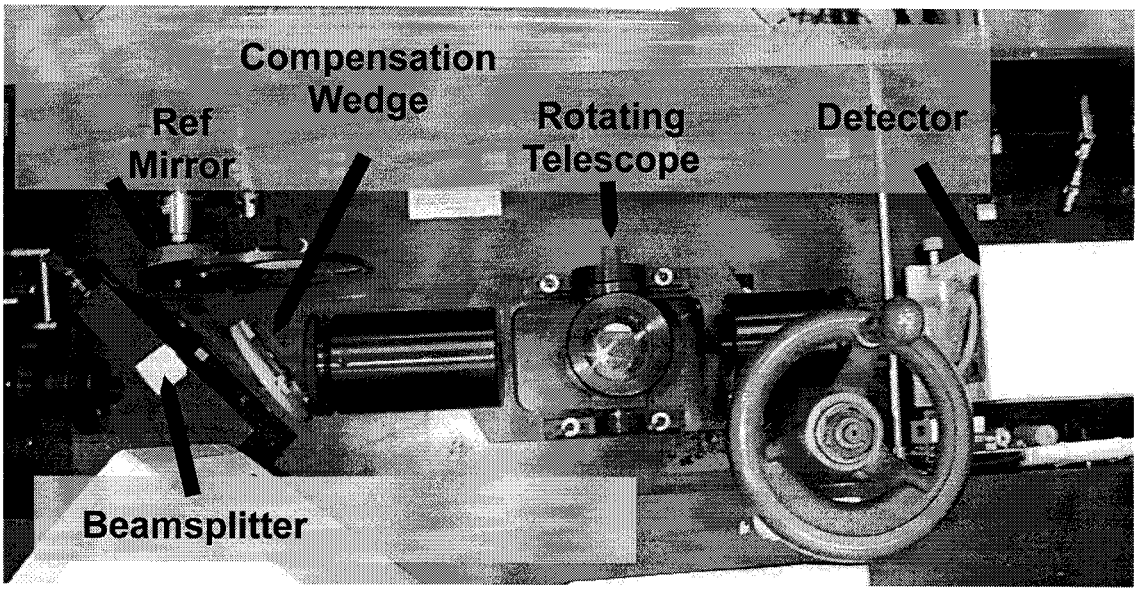

Figure 8: Modified BRO IR PSI

4. IR SHACK-HARTMANN WAVEFRONT SENSOR

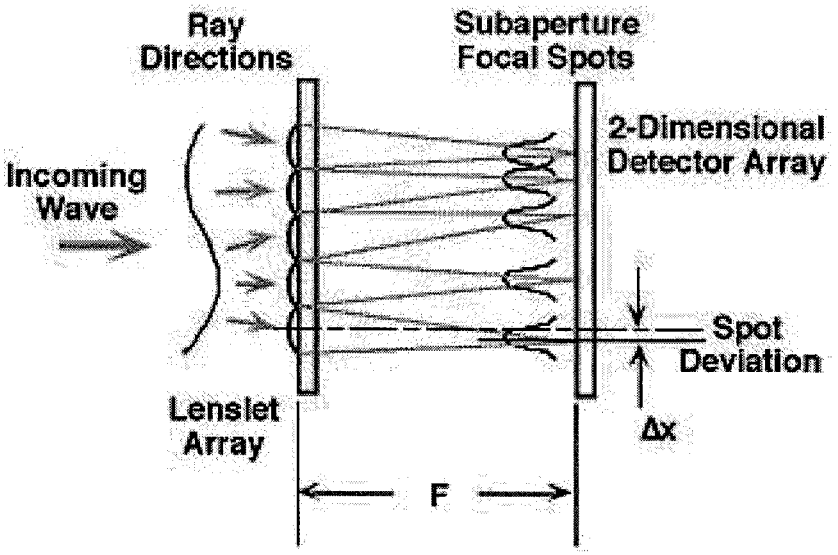

Figure 9: Principle of Operation for a Shack-Hartmann Sensor (Courtesy AOA Incorporated)

The Shack-Hartmann sensor operates by using a Micro Lens Array (MLA or lenslet array) located at an image of the system pupil to sample segments of the wavefront under test (see Figure 9). These wavefront samples are focused on a CCD array. For each lens in the MLA there is region of the CCD that is used to measure the centroid of the spot produced by that lens. Typically a 1:1 relay is used to re-image the MLA spots onto the CCD array. In that case the pixels that lie in the shadow of each MLA lens are those used for that lens' centroiding measurement. To establish a calibration for the expected centroid position for each site a well-corrected reference mirror is used. The measurement process consists of two steps:

1. Measure the centroids of the reference mirror's spots

2. Measure the centroid of the test mirror's spots.

The centroid location offset between these two measurements is a measure of the average wavefront slope at the corresponding lens in the MLA. The resulting set of wavefront slope measurements are then used to synthesize the wavefront of the optical system being tested.

Shack-Hartmann wavefront sensors are available from commercial manufacturers (e.g. Wavescope from AOA Incorporated). However, the commercial sensors did not meet the needs for the test. The primary issue was the use of visible light. The surface roughness of the 2 m demonstration mirror met the requirements for the Herschel Space Observatory. However, it was excessive for use with a visible Shack-Hartmann sensor.

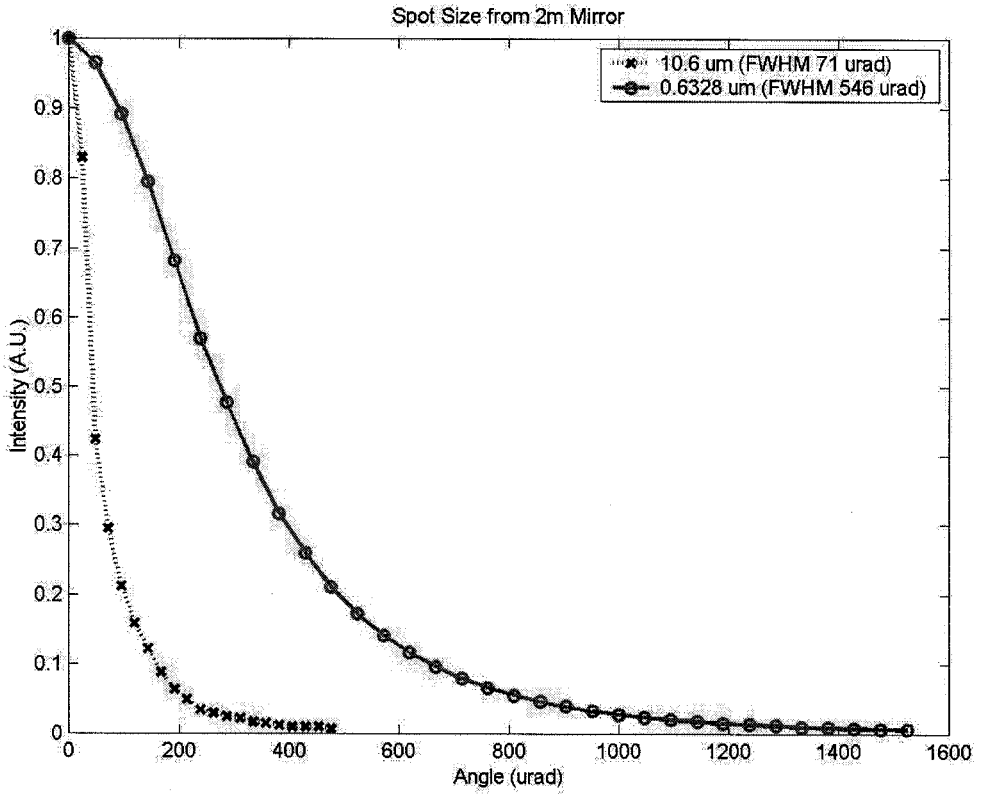

Figure 10: Spot Size Measurements from 2m Demonstration Mirror

Excessive surface roughness can cause extremely large spots in the focal plane of the lens array. The result is noise from adjacent spots can interfere with the centroid calculation. In order to quantify this effect, the spot size produced by the 2 m demonstration mirror was measured at two wavelengths: 0.6328 μm and 10.6 μm and this data are shown in Figure 10. The spot size for λ = 10.6 μm is much smaller than the spot size for λ = 0.6328 μm. For this reason, an infrared source was preferred. Essentially, increasing the wavelength from 0.6 μm to 10.6 μm relaxed the requirement on surface roughness for

proper centroid calculation. The goal of the modification to infrared was to leave as much of the AOA Wavescope (hardware and software) intact and merely change the illumination source, optics train, and sensor (see Figure 11).

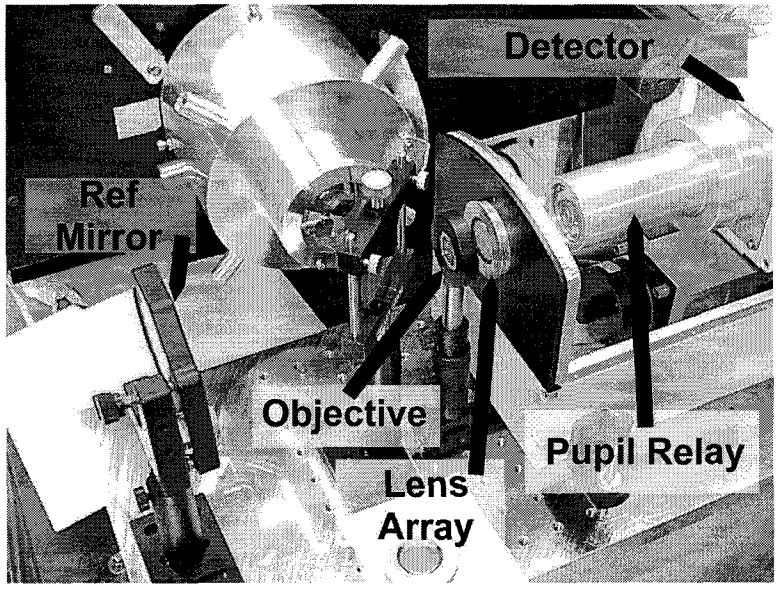

Figure 11: Modifications to Infrared Shack-Hartmann Sensor (IR SH)

The lens array for the IR SH was manufactured from KRS-5. Lens arrays are common components for visible applications. However, the options for infrared (10.6 μm) are limited. Technologies used to create visible lens arrays include: stamping/molding, diffraction optics, index doping, and flowing. Of these options, only molding and diffractive optics were considered for this application. The delivery time on diffractive optics for the infrared was too long to meet the schedule. KRS-5 was identified by AOA as a material compliant enough to be molded using existing tooling. A variety of lens arrays with various F/#'s and lens diameters were manufactured. The number of lenses in the array is equal to the number of sample points of the wavefront. The size of each lens is proportional to the number of lenses in the array. Finally, the focal length of each lens is proportional to the diffraction limited spot size and therefore the accuracy of the slope (spot centroiding) calculation. Given practical limitations and existing tooling, a limited number of lens arrays were fabricated (see Table 2).

Table 2: KRS-5 Lens Arrays Available

Lenslet Array	Focal Length	Lens Diam	N_{pts}
1	2.8 mm	0.3 mm	40
2	3.7 mm	0.5 mm	24
3	7.4 mm	0.5 mm	24

As in the interferometer, both an objective lens and an image relay telescope were necessary for operation. The objective lens used to image the return signal to the MLA was a ZnSe singlet and the image relay was a telecentric (1:1) telescope constructed with two plano-convex singlets.

Although the light source need not be coherent, the laser from the IR PSI was chosen to illuminate the mirror. The F/2 objective lens designed for the IR PSI was used to generate a point source for the illumination of the mirror.

The sensor for the IR SH was a room temperature microbolometer array camera, identical to the model used in the IR PSI.

5. TEST CONFIGURATION

The configuration for the instruments had to meet several criteria:

- Fit within the small footprint allocated for metrology equipment at the test facility
- Shared light source (CO_2 laser),
- Shared aperture to the chamber,
- Sequential measurement,
- Rapid switchover between instruments.

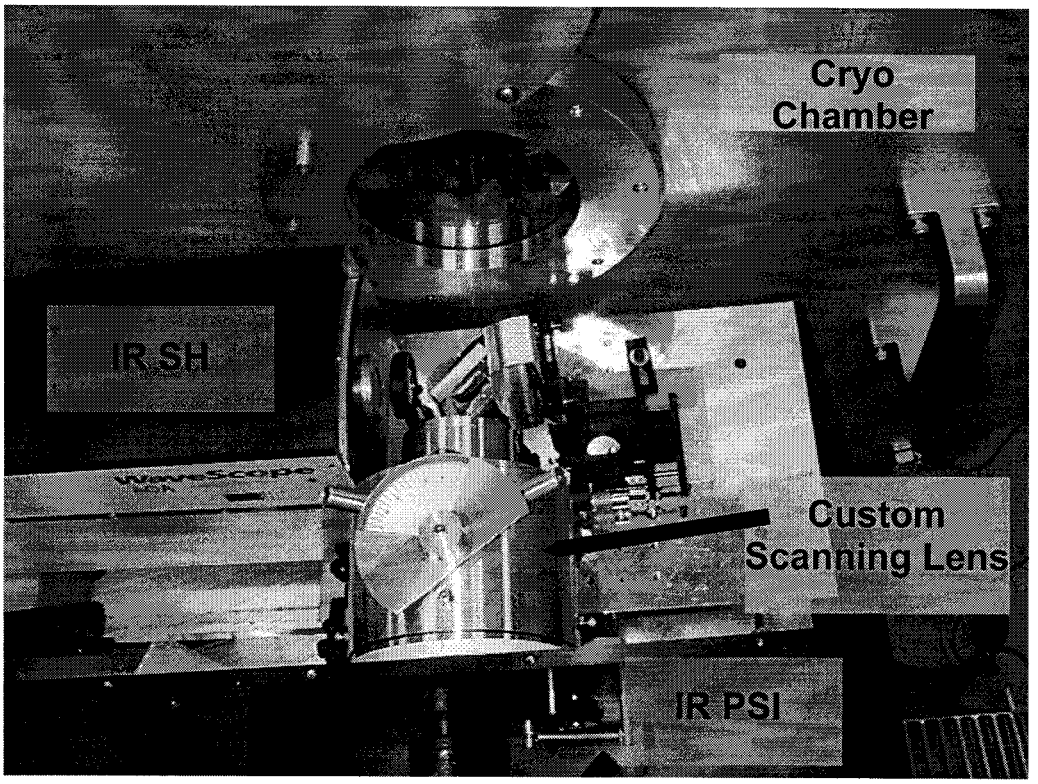

Figure 12: Photograph of Instrument Configuration

These goals were achieved in the configuration shown in Figure 12. The IR PSI was aligned to the same axis as the 2 m demonstration mirror. The IR SH was aligned at 90 degrees. Across from the IR SH was a reference mirror. The reference mirror was a necessary reference for the operation of the IR SH. A beam splitter was inserted between the four arms of the configuration to provide easy access from either instrument to the mirror under test or the reference mirror.

6. METROLOGY CAPABILITY

1. Infrared Phase Shifting Interferometer (IR PSI)

The key performance criteria for the IR PSI were:

- High Lateral Resolution
- High Slope Error Cutoff
- Minimal Sensitivity to Vibrations

- High Accuracy
- Minimal Random Errors

The lateral resolution was measured by placing a tilting reference mirror external to the interferometer. A maximum of 60 fringes (line pairs) across the clear aperture could be recorded before there is a loss in signal. This corresponds to between 5 and 6 pixels per fringe. Each pixel is approximately 51 μm x 51 μm, yielding a resolution of 250 – 300 μm. According to the ray tracing model of the interferometer, the diffraction limited performance of the interferometer optical system is 150 μm and the MTF is 50% at a resolution of 80 fringes across the detector. The resolution of 60 fringes (line pairs) across the aperture corresponds to a resolution of 16 mm on the 2 m demonstration mirror.

The slope error cutoff is directly related to the maximum fringe density that limits the lateral resolution. The 60 fringes across the aperture corresponds to 30 waves (10.6 μm) of surface error over 2000 mm. This corresponds to 160 μrad slope error for the 1X magnification, 320 μrad slope error for the 2X magnification, and 640 μrad slope error for the 4X magnification.

The sensitivity to vibration was limited by the magnitude and frequency of the vibrations. The data collection rate was limited by the frame grabbing hardware and the number of buckets in the phase shifting algorithm. The data collection rate was approximately 9 seconds for each surface. The video rate was 30 fps. Therefore the interferometer was sensitive to any disturbances between 30 Hz and 0.1 Hz. Dynamic measurements in the test apparatus were used to monitor disturbances and correlate these with activities at the facility. [15]

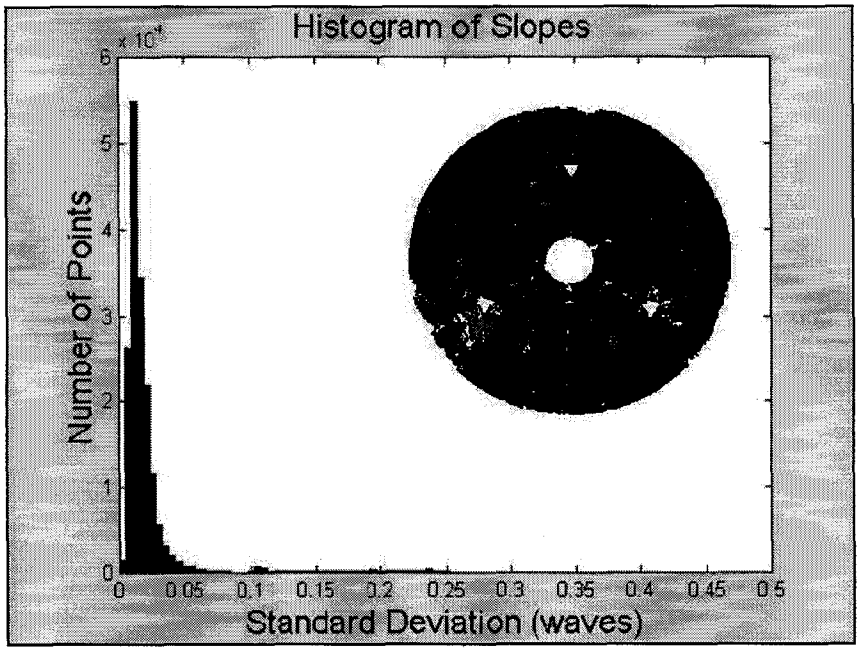

Figure 13: Histogram of Random Errors in Mirror Surface Measurement (1 σ of errors < λ/50 = 0.2 μm)

The random errors were minimized by averaging several (up to 30) surfaces. These errors were characterized in a variety of environments (optical laboratory and cryo test facility). The errors were evaluated by collecting 30 surfaces and calculating the average and standard deviation of the surface value for each pixel representing the surface of the mirror. A histogram was then generated for all the pixels across the surface (see Figure 13). Although a few points exhibit large errors (λ/4), the overwhelming majority of the points across the mirror surface, even at 70 K, were repeatable to better than λ/50 (0.2 μm).

2. Infrared Shack-Hartmann (IR SH)

The key performance criteria for the IR SH were the same as the interferometer:

- High Lateral Resolution
- High Slope Error Cutoff
- Minimal Sensitivity to Vibrations
- High Accuracy
- Minimal Random Errors

The constraints on the performance a Shack-Hartman wavefront sensor are unique. Using a relatively simple set of equations based on the number of lenses in the array, the diffraction limited spot size of the lenses in the array, and the number of pixels on the detector, a model for the resolution and accuracy of the sensor can be created:

$$M_{mirror} = \frac{s_{lenslet}}{s_{mirror}},$$

$$s_{mirror} = R_{mirror} + f_{obj}, \quad \frac{1}{s_{lenslet}} = \frac{1}{f_{obj}} - \frac{1}{s_{mirror}}, \quad f_{obj} = \left(\frac{R_{mirror}}{D_{mirror}}\right) D_{sensor}$$

$$\theta_{err} \cong \left(C_{centroid} \frac{\delta_{pixel}}{f_{lenslet}}\right) M_{mirror}, \quad \theta_{\max} \cong \frac{D_{lenslet}/2}{f_{lenslet}} M_{mirror},$$

$$N_{pts} = \frac{D_{sensor}}{D_{lenslet}}, \quad \delta_{PV} = \frac{D_{lenslet}\theta_{err}}{M_{mirror}},$$

where M_{mirror} (6×10^{-3}) is the magnification of the mirror pupil onto the sensor, s_{mirror} (4.225 m) distance between objective and the mirror, $s_{lenslet}$ (25.4 mm) is the distance between the objective and the lenslet, f_{obj} (25.2 mm) is the objective lens focal length, R_{mirror} (4.2 m) is the radius of curvature of the mirror, D_{mirror} (2 m) is the diameter of the mirror, D_{sensor} (12 mm) is the size of the pixilated detector, θ_{err} is the error in the surface slope measurement, $C_{centroid}$ (0.10) is the accuracy of the centroiding operation expressed as a fraction of a pixel, δ_{pixel} (50 μm) is the diameter of a pixel on the sensor, $f_{lenslet}$ is the focal length of the lenslet, θ_{max} is the maximum surface slope that allows a spot to fall within the view of a single lens in the lenslet array, $D_{lenslet}$ is the diameter of a single lens in the lenslet array, N_{pts} is the number of data points (i.e. number of lenses across the lenslet array) collected across the aperture of the mirror, and δ_{pv} is an estimate of the error in surface height measurement. This model assumes a 1:1 relay of the image of the spots to the sensor and an objective that magnifies the mirror pupil to match precisely the size of the sensor. Using this model and the parameters for the instrument, the performance can be reviewed in Table 3.

Table 3: IR SH Predicted Performance

Lenslet Array	Focal Length	Lens Diam	θ_{err}	θ_{max}	δ_{PV}	N_{points}
1	2.8 mm	0.3 mm	11 μrad	320 μrad	0.55 μm	40
2	3.7 mm	0.5 mm	8.3 μrad	400 μrad	0.69 μm	24
3	7.4 mm	0.5 mm	4.1 μrad	200 μrad	0.34 μm	24

From these options, the third lens array was eliminated due to the small dynamic range (θ_{max} too small). The first lens array was desirable because of the number of data points collected across the aperture and the high dynamic range. The second lens array offered an increased dynamic range.

Table 4: Viewing Area of Lenses in Lenslet Array in Practice

Lenslet Array	No. Lenses Across Full Aperture	Area on Mirror Sampled by Each Lens
1	30	67 mm
2	18	111 mm
3	18	111 mm

When reduced to practice, the results indicate that the IR SH was a difficult technique to use for mirrors with quilting (mid-spatial frequencies). The principle of the Shack-Hartmann instrument relies on isoplanatic regions equal in size to the area observed by each lens element. Expressed in another way, the technique yields the most accurate results when the wavefront aberration over each lens element is small. When the aberrations are large over a single lens, the spots in the focal plane of the lens array are misshapen and the centroiding operation is no longer accurate. Table 4 shows the lens arrays and the size they sample of the mirror. The cells that comprise the ribs in the mirror under test were approximately 105 mm in diameter. Even at the highest density lens array, there were less than two lens arrays per cell on the mirror. Although the quilting was not consistent [15], there was sufficient surface deformation to disrupt the focal spots.

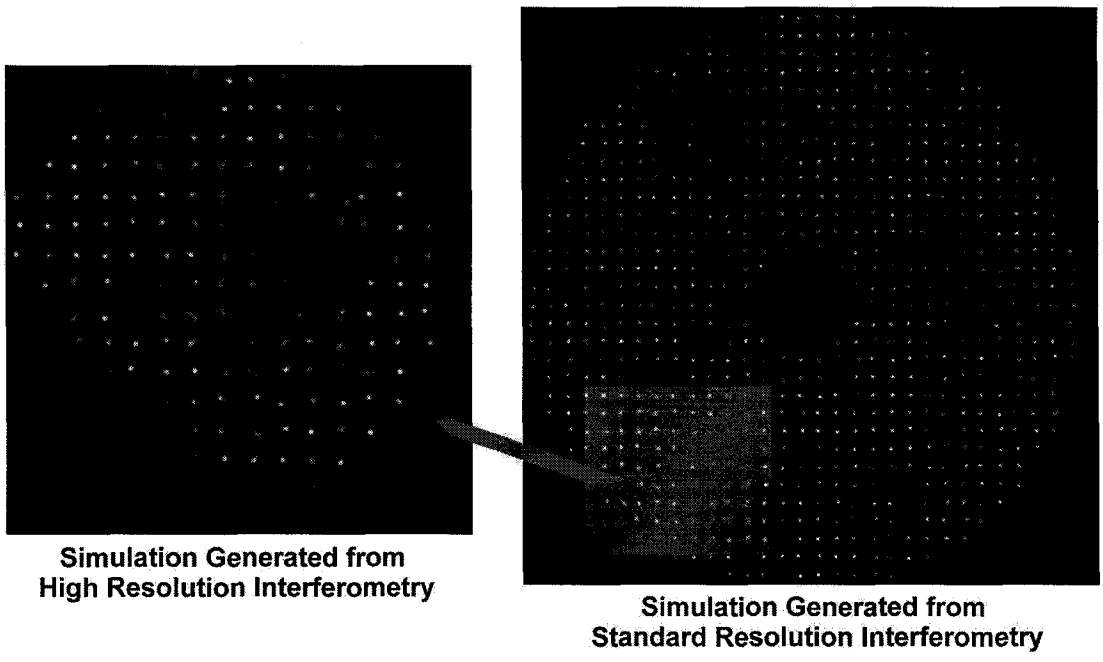

Figure 14: Simulated Spots from IR SH at 70 K

To illustrate this challenge, a simulation of the IR SH was conducted and compared with the experimental results. Surface data from the interferometric measurements at 70 K were used to create the wavefront. The wavefront was segmented into an array and the spots were calculated using a FFT algorithm. Figure 14 shows two simulations of the Shack-Hartmann spots: one generated from full aperture data (right) and one generated from high resolution sub aperture data (left). Notice that the spots on the right appear to be well behaved. However, when the high resolution interferometry surface measurement is used to generate the same spots, they appear severely distorted in several locations. Figure 15 show the data collected from the IR SH at room temperature and 100 K. Notice that the spots appear to be severely distorted. The conclusion from this exercise is that for this surface, high resolution data is necessary to accurately simulate the Shack-Hartmann sensor. Unfortunately, the software used for the IR SH was unable to generate a satisfactory surface map using the data shown in Figure 15.

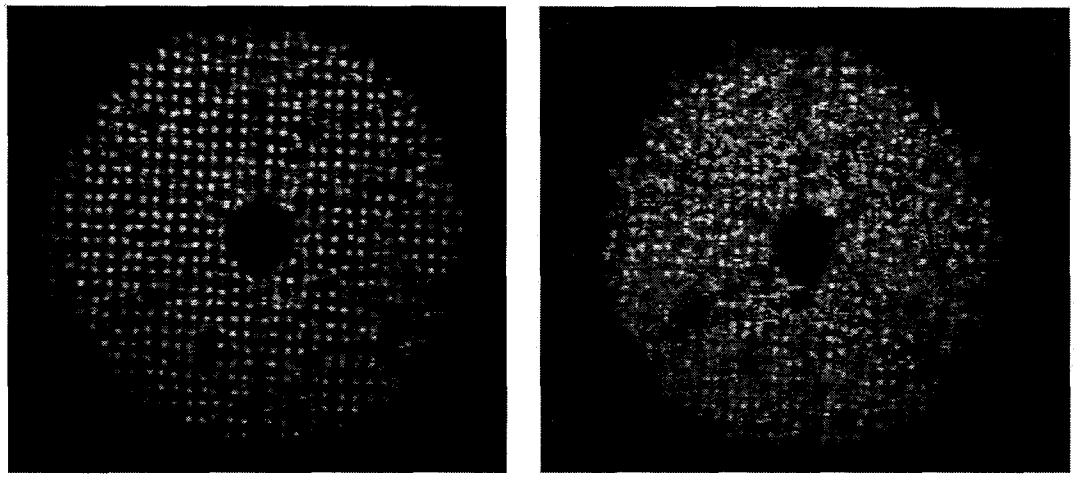

Figure 15: Spots Recorded for Mirror at Room Temperature and at 100 K

The authors recommend that care be taken when using a Shack-Hartmann wavefront sensor to test an optic with spatial frequency errors close to the sampling of the lens arrays. When quilting or other aberrations with mid to high spatial frequencies are anticipated, these can significantly disrupt the spots in this type of sensor. The simulations of the Shack-Hartmann sensor demonstrate that predicting the success of this type of test may rely heavily on the resolution of the previously collected data. If this type of sensor is used to measure a highly aberrated wavefront, the lens array density should be high enough to guarantee high Strehl ratio spots. In the presence of quilting, at least five (5) lenses should be used to cover each cell of the quilted mirror. The aforementioned formulas indicate that merely increasing the number of lenses without increasing the number of pixels in the sensor will compromise the accuracy of the instrument. Therefore the number of pixels on the sensor would need to increase by a factor of five (5) as well.

7. SUMMARY

A unique all carbon fiber composite telescope primary mirror has been described. This mirror and its potential application to telescopes like the Herschel Space Observatory inspired the characterization of its surface errors at cryogenic temperatures. This characterization effort resulted in a survey of suitable optical measurement techniques. Two instruments were selected: an infrared phase shifting interferometer and an infrared Shack-Hartmann wavefront sensor. Existing commercial instruments were adapted using the methods described and their performance was evaluated. The Shack-Hartmann wavefront sensor was not well suited for testing this mirror. Surface errors with spatial frequencies that were close to the period of the lens array caused aberrations that made the data difficult to reduce to a surface measurement. For this optical test, the phase shifting interferometer proved superior in accuracy, dynamic range, and lateral resolution. The interferometer provided all of the data necessary for full characterization.

8. ACKNOWLEDGEMENTS

The work described in this paper was carried out by COI, LWO and JPL (California Institute of Technology), under a contract with the National Aeronautics and Space Administration. The authors wish to thank Pat Woida for his hard work in refurbishing the Wyko and BRO interferometers and for his continued consultation on interferometry, Marty Levine (formerly with AOA Incorporated now with JPL) for efforts regarding the manufacturing of the KRS-5 lenslet arrays and many valuable discussions about the Wavescope tool, and Raymond Castonguay for his contributions and rapid modifications to the Intelliwave software from Engineering Synthesis Design.

9. REFERENCES

1. E. J. Cohen, S. J. Connell, K. J. Dodson, J. L. Abbot, A. Abusafieh, Z. Backovsky, J. Dyer, J. Escobedo-Torres, Z. Friedman, A. Hull, D. Small, P. Thorndyke, and S. Whitmore "Architecture of the FIRST telescope," SPIE Proceedings Vol 4015, March 2000.
2. S. J. Connell, K. J. Dodson, Z. Friedman, B. Catanzaro, S. Whitmore, and E. J. Cohen "Design progression of an all-composite primary mirror for the FIRST Telescope," SPIE Proceedings Vol 4013, March 2000.
3. B. Catanzaro, J. Thomas, S. Backovsky, D. Barber, D. Small, R. Johnston, and E. J. Cohen "The effects of aberrations (low order and quilting) on the performance of the all-composite design for the Herschel Space Observatory," SPIE Proceedings Vol 4444, August 2001.
4. N. Ninane "On ground verification of high precision antenna structures", Report No. RP-CSL-FIR-93006, 1993.
5. E. Hochberg, "Optical figure testing of prototype mirrors for JPL's Precision Segmented Reflector (PSR) program," Active and adaptive optical systems; Proceedings of the Meeting, in San Diego, July, 1991.
6. P. Woida, W. Hoffman, S. Connell, and E. Kasl "Low-temperature figure stability of a COI all-composite mirror M4," SPIE Proceedings Vol 3430, December 1998.
7. Optical Shop Testing, D. Malacara, Wiley and Sons, January 1992.
8. F. J. Roddier "Wavefront curvature sensing and compensation methods in adaptive optics," SPIE Proceedings Vol 1487, July 1991.
9. M. J. Northcott, J. Graves, F. J. Roddier, and F. Rigaut "Design and performance of an 85-actuator curvature system," SPIE Proceedings Vol 4007, July 2000.
10. D. Redding, S. Basinger, A. Lowman, A. Kissil, P. Bely, R. Burg, R. Lyon, G. Mosier, M. Femiano, M. Wilson, G. Schunk, L. Craig, D. Jacobson, J. Rakoczy, and J. Hadaway "Wavefront sensing and control for a Next-Generation Space Telescope," SPIE Proceedings Vol 3356, August 1998.
11. C. Bowers, P. Davila, B. Dean, B. Perkins, M. Wilson, D. Redding, S. Basinger, D. Cohen, A. Lowman, F. Shi, L. Burns, M. Fitzmaurice. T. Norton, P. Petrone, and L. Wheeler "Initial test results from the Next Generation Space Telescope (NGST) wavefront sensing and control testbed (WCT)," SPIE Proceedings Vol 4013, July 2000.
12. Introduction to Wavefront Sensors, J. Geary, SPIE Press, June 1995
13. G. Mehle, K. Dodson, and E. Ruch "Recent developments in hybrid mirror technology for the Next Generation Space Telescope," SPIE Proceedings Vol 4013, July 2000.
14. J. Mayo, L. DeHainaut, K. Bell, W. Smith, D. Kilpatrick, and R. Dyer "Ultralightweight optics for space applications," SPIE Proceedings Vol 4013, July 2000.
15. B. Catanzaro, S. Connell, M. Mimovich, Z. Backovsky, G. Williams, J. A. Thomas, D. Barber, R. Johnston, J. Hylton, K. Dodson, and E. Cohen "Cryogenic (70K) measurement of an all-composite 2-meter diameter mirror," SPIE Proceedings Vol 4444, Aug 2001.